

CLAS: DOUBLE-PION BEAM ASYMMETRY

S. STRAUCH FOR THE CLAS COLLABORATION

University of South Carolina
Department of Physics and Astronomy
712 Main Street
Columbia, SC 29208, USA
E-mail: strauch@sc.edu

Beam-helicity asymmetries for the $\bar{\gamma}p \rightarrow p\pi^+\pi^-$ reaction have been measured for center-of-mass energies between 1.35 GeV and 2.30 GeV at Jefferson Lab with the CEBAF Large Acceptance Spectrometer using circularly polarized tagged photons. The beam-helicity asymmetries vary with kinematics and exhibit strong sensitivity to the dynamics of the reaction, as demonstrated in the comparison of the data with results of various phenomenological model calculations. These models currently do not provide an adequate description of the data over the entire kinematic range covered in this experiment. Additional polarization observables are accessible in an upcoming experiment at Jefferson Lab with polarized beam and target.

1. Introduction

The properties of the excited states of baryons reflect the dynamics and relevant degrees of freedom within them. The study of nucleon resonances is thus an important avenue to learn about the strong interaction. To disentangle and study experimentally these many, mostly weak, and largely overlapping resonances is a challenging task, especially at higher energies. Many nucleon resonances in the mass region above 1.6 GeV decay predominantly through either $\pi\Delta$ or ρN intermediate states into $\pi\pi N$ final states (see the Particle-Data Group review¹). This is the region where resonances are predicted by symmetric quark models, but have not been observed in the πN channel (the so-called “missing” resonances); yet may couple strongly to channels like $\pi\Delta$.² This makes electromagnetic double-pion production an important tool in the investigation of the structure of the nucleon and the most promising approach is to employ polarization degrees of freedom in the measurement. There exist a rather large amount of unpolarized cross-section data of double-pion photo- and electroproduction on the proton;³ the amount of polarization observables in these reactions,

however, remains quite sparse.⁴

The CLAS Collaboration published recently beam-helicity-asymmetry data in the $\bar{\gamma}p \rightarrow p\pi^+\pi^-$ reaction for energies W between 1.35 GeV and 2.30 GeV in the center of mass, where the photon beam is circularly polarized and neither target nor recoil polarization is specified.⁵ These novel data combine the study of the double-pion final state with the sensitivity of polarization observables. The beam-helicity asymmetry is one of 64 polarization observables in the $\bar{\gamma}p \rightarrow p\pi^+\pi^-$ reaction and is defined as⁶

$$I^\odot = \frac{1}{P_\gamma} \cdot \frac{\sigma^+ - \sigma^-}{\sigma^+ + \sigma^-}, \quad (1)$$

where P_γ is the degree of circular polarization of the photon and σ^\pm are the cross sections for the two photon-helicity states $\lambda_\gamma = \pm 1$.

In this contribution, we give a brief overview of our data, compare with results of phenomenological models, demonstrate the sensitivity of this observable to the dynamics of the reaction, and give an outlook on further studies of other polarization observables.

2. Experiment

The $\bar{\gamma}p \rightarrow p\pi^+\pi^-$ reaction was studied with the CEBAF Large Acceptance Spectrometer (CLAS)⁷ at Thomas Jefferson National Accelerator Facility (Jefferson Lab). A schematic view of the reaction, together with angle definitions, is shown in Fig. 1. Longitudinally polarized electrons with

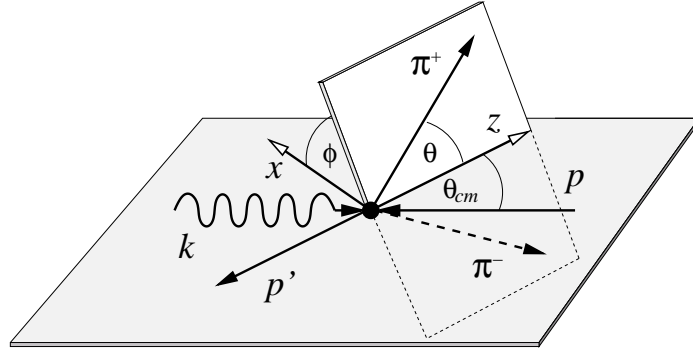


Figure 1. Angle definitions for the circularly polarized real-photon reaction $\bar{\gamma}p \rightarrow p\pi^+\pi^-$; θ_{cm} is defined in the overall center-of-mass frame, and θ and ϕ are defined as the π^+ polar and azimuthal angles in the rest frame of the $\pi^+\pi^-$ system with the z direction along the total momentum of the $\pi^+\pi^-$ system (helicity frame).

an energy of 2.445 GeV were incident on the thin radiator of the Hall-B Photon Tagger⁸ and produced circularly-polarized tagged photons in the energy range between 0.5 GeV and 2.3 GeV. The collimated photon beam irradiated a liquid-hydrogen target. The circular polarization of the photon beam was determined from the electron-beam polarization and the ratio of photon and incident electron energy.⁹ The degree of photon-beam polarization varied from ≈ 0.16 at the lowest photon energy up to ≈ 0.66 at the highest energy. The $\bar{\gamma}p \rightarrow p\pi^+\pi^-$ reaction channel was identified in this kinematically complete experiment by the missing-mass technique, requiring either the detection of all three final-state particles or the detection of two out of the three particles in the CLAS detector.

A total of 3×10^7 $p\pi^+\pi^-$ events were accumulated. Experimental values of the helicity asymmetry were then obtained as

$$I_{\text{exp}}^{\odot} = \frac{1}{\bar{P}_{\gamma}} \cdot \frac{Y^+ - Y^-}{Y^+ + Y^-}, \quad (2)$$

where Y^{\pm} are the experimental yields, corrected for a small electron-beam-charge asymmetry. The experimental asymmetries have not been corrected for the CLAS acceptance to avoid systematic uncertainties. Instead, the data are compared with event-weighted mean values of asymmetries from model calculations. These mean values of asymmetries in a kinematical bin are given by

$$\bar{I}_{\text{model}}^{\odot} = \frac{1}{\bar{P}_{\gamma}} \cdot \frac{1}{N} \sum_{i=1}^N P_{\gamma,i} I_i^{\odot}, \quad (3)$$

where the sum runs over all N events observed in that bin; $P_{\gamma,i}$ and I_i^{\odot} are the degree of circular beam polarization and the model asymmetry, respectively, for the kinematics of each of those events. The only major source of systematic uncertainty is the degree of the beam polarization, which is known to about 3%. The uncertainty from the beam-charge asymmetry is negligible (less than 10^{-3}).

3. Results

Figure 2 shows ϕ -angular distributions of the helicity asymmetry for various selected 50-MeV-wide center-of-mass energy bins between $W = 1.40$ GeV and 2.30 GeV. The data are integrated over the full CLAS acceptance. The analysis shows large asymmetries which change markedly with W up to 1.80 GeV; thereafter they remain rather stable. The asymmetries are

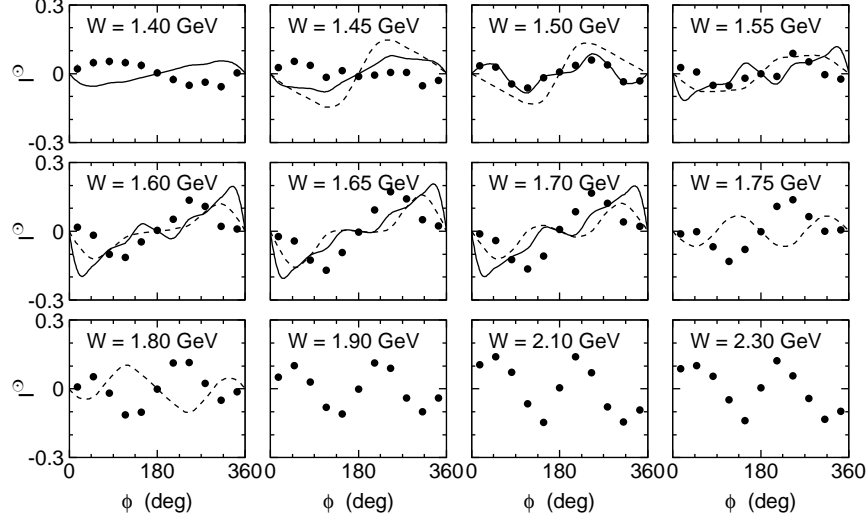


Figure 2. Angular distributions for selected center-of-mass energy bins (each with $\Delta W = 50$ MeV) of the beam-helicity asymmetry for the $\bar{\gamma}p \rightarrow p\pi^+\pi^-$ reaction. The data are integrated over the detector acceptance. The statistical uncertainties are smaller than the symbol size. The dashed and solid curves are the results from model calculations by Mokeev *et al.*¹⁰ (for $1.45 \text{ GeV} \leq W \leq 1.80 \text{ GeV}$), and by Fix and Arenhövel¹¹ (for $W \leq 1.70 \text{ GeV}$), respectively.

odd functions of ϕ and vanish for coplanar kinematics ($\phi = 0$ and 180°), as expected from parity conservation.⁶ Thus only sine terms contribute to the Fourier expansion of these distributions, $\sum a_k \sin(k\phi)$. If two of the final-state particles are identical, like in the $\pi^0\pi^0p$ final state, the form of the angular distributions is further restricted and only even-order terms enter the Fourier series. This has indeed been observed by the CLAS collaboration in beam-helicity asymmetry data in the $\bar{\gamma}^3\text{He} \rightarrow ppn$ reaction, where the lowest order term is $a_2 \sin(2\phi)$.¹²

The data are compared with results of available phenomenological models. In the approach by Mokeev *et al.*¹⁰ (dashed curves), double-charged-pion photo- and electroproduction are described by a set of quasi-two-body mechanisms with unstable particles in the intermediate states: $\pi\Delta$, ρN , $\pi N(1520)$, $\pi N(1680)$, $\pi\Delta(1600)$ and with subsequent decays to the $\pi^+\pi^-p$ final state. Residual direct $\pi^+\pi^-p$ mechanisms are parametrized by exchange diagrams. The model provides a good description of all available CLAS cross-section and world data on double-pion photo- and electroproduction at $W < 1.9 \text{ GeV}$ and $Q^2 < 1.5 \text{ GeV}^2$. Results have also been

obtained by Fix and Arenhövel using an effective Lagrangian approach with Born and resonance diagrams at the tree level.¹¹ The corresponding results are shown in Fig. 2 as solid curves.

Although both models previously provided a good description of unpolarized cross sections, neither of the models give a reasonable description of the present beam-asymmetry data over the entire kinematic range covered in this experiment. Even though the model predictions agree remarkably well for certain conditions, for other conditions they are much worse and sometimes even out of phase entirely.

The result of a Fourier analysis of the ϕ distributions is shown in Fig. 3 and compared with model calculations by Fix and Arenhövel.¹¹ Apart of the $W = 1.4$ GeV region, excellent agreement is achieved in these calculations for the a_1 coefficient; yet the distribution of the a_2 coefficients deviates from the data above $W \approx 1.55$ GeV. It would be interesting to find out if there are specific reaction mechanisms contributing to specific terms in the Fourier decomposition of the angular distributions.

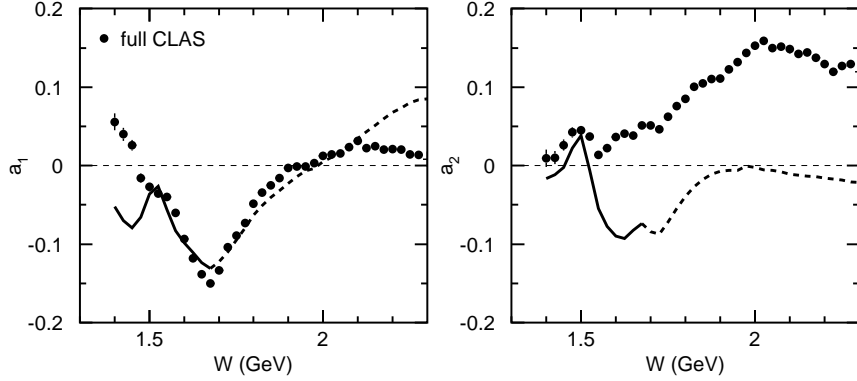


Figure 3. First (a_1) and second (a_2) order Fourier components of the beam-helicity asymmetry as a function of the γp center-of-mass energy. The data are integrated over the full CLAS acceptance and compared with model calculations by Fix and Arenhövel¹¹ within (solid) and outside (dashed) the range of validity of that model ($W < 1.7$ GeV).

The main theoretical challenge for double-pion photoproduction lies in the fact that several subprocesses may contribute, even though any given individual contribution may be small. In his recent work Roca¹³ studies the beam-helicity asymmetry and our preliminary data¹⁴ in the framework of the Valencia model for double-pion photoproduction. He shows that the

shape and strength of the asymmetries depend strongly on the internal mechanisms and interferences among different contributions to the process. In this connection, the polarization measurements should be very helpful in separating the individual terms. The particular sensitivity of the beam asymmetry to interference effects among various amplitudes is illustrated in Fig. 4. The solid, dashed, dotted, and dash-dotted curves are the re-

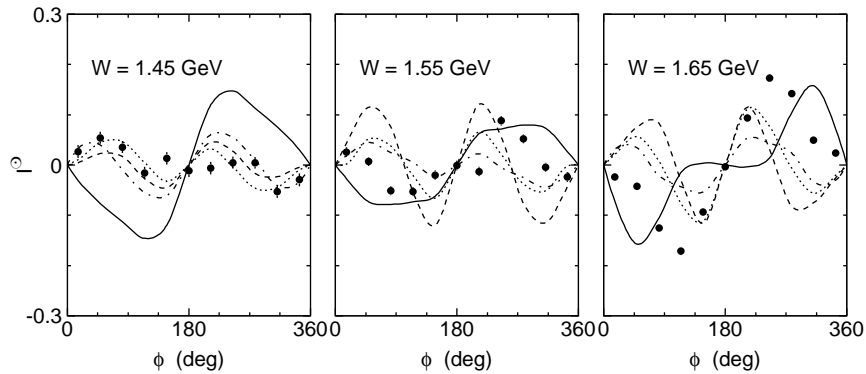


Figure 4. Integrated angular distributions for selected center-of-mass energy bins (each with $\Delta W = 50$ MeV) of the beam-helicity asymmetry for the $\vec{\gamma}p \rightarrow p\pi^+\pi^-$ reaction. The solid, dashed, dotted, and dash-dotted curves are results from model calculations by Mokeev *et al.*¹⁰ with relative phases of 0, $\pi/2$, π , and $3\pi/2$ between the background- and $\pi\Delta$ -subchannel amplitudes, respectively.

sults from model calculations by Mokeev *et al.*¹⁰ with relative phases of 0, $\pi/2$, π , and $3\pi/2$ between the background- and $\pi\Delta$ -subchannel amplitudes, respectively; in this model initial- and final-state interactions are treated effectively and allow for those relative phases. The access to interference effects permit a cleaner separation of background and resonances. This in turn makes it possible to make more reliable statements about the existence and properties of nucleon resonances.

The large number of observed $\vec{\gamma}p \rightarrow p\pi^+\pi^-$ events allows for a confident analysis of the data in selected kinematic regions, making it possible to tune the different parts of the production amplitude independently. Figures 5 and 6 give two examples of more selective distributions of the same data around $W = 1.50$ GeV binned into nine bins in the invariant mass $M(p\pi^+)$ and into nine bins in the invariant mass $M(\pi^+\pi^-)$, respectively.

The double-pion final state allows further the study of sequential decays of nucleon resonances such as $N(1520) \rightarrow \pi\Delta \rightarrow \pi\pi N$. Figure 7 shows the

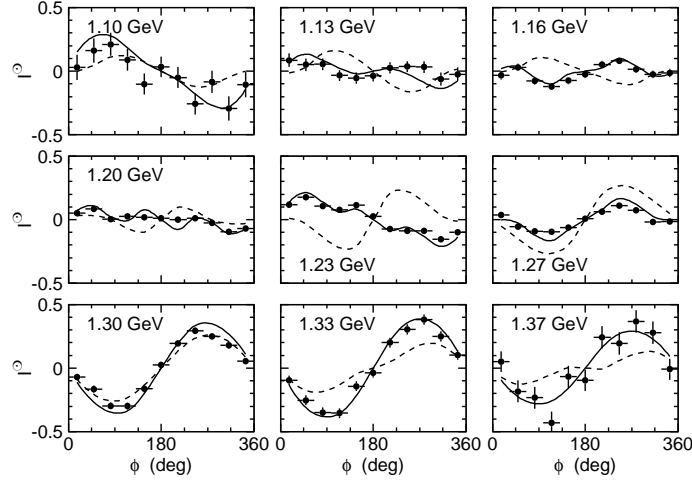


Figure 5. Helicity asymmetries at $W = 1.50$ GeV for nine bins of the invariant mass $M(p\pi^+)$ with its mean values indicated in each panel. The asymmetries are otherwise integrated over the full CLAS acceptance. The solid curves are the results of Mokeev *et al.*;¹⁰ the dashed curves show results of calculations by Fix and Arenhövel.¹¹

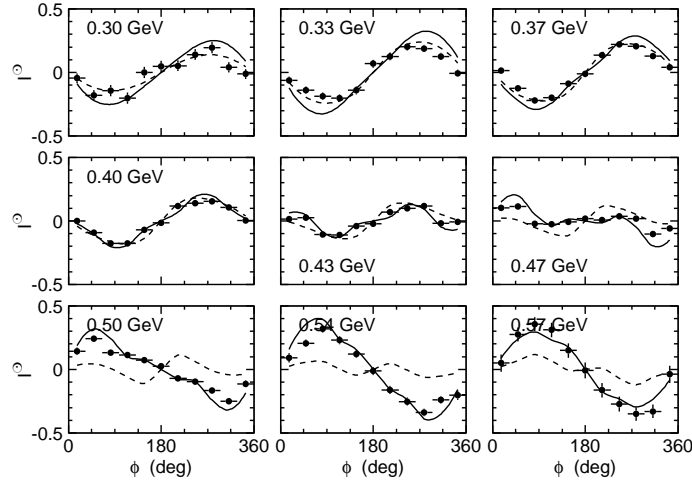


Figure 6. Same as Fig. 5 for nine bins of the invariant mass $M(\pi^+\pi^-)$.

Fourier coefficients a_1 and a_2 of the ϕ angular distributions as a function of the invariant mass $M(p\pi^-)$ for $W = 1.520$ GeV. The most interesting feature of these data is the change that occurs as $M(p\pi^-)$ traverses the

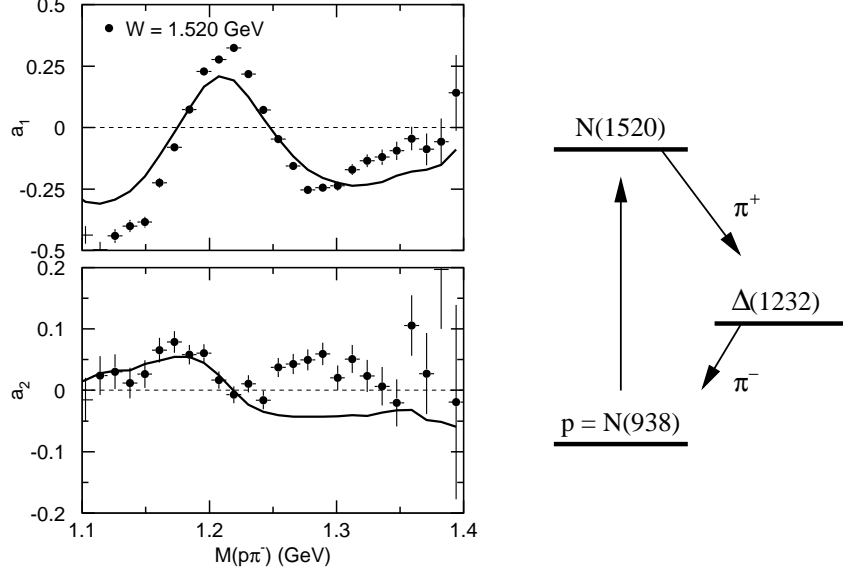


Figure 7. Fourier coefficients a_1 and a_2 as a function of the invariant mass $M(p\pi^-)$ for $W = 1.520$ GeV. The curves are the results of Fix and Arenhövel.¹¹ The vertical line indicates the masses of the Δ resonance. The diagram illustrates the sequential decay $N(1520) \rightarrow \pi^+\Delta^0 \rightarrow \pi^+\pi^-p$ which might be observed in the data.

$\Delta(1232)$ resonance. A maximum is seen in the region of this resonance. This hints at the way in which the helicity asymmetry (along with other polarization observables) could be used in studies of baryon spectroscopy.

4. Outlook and Summary

The observable I^\odot discussed here is only one of many polarization observables in the double-pion photoproduction reaction. Many more polarization observables will be accessible in a proposed experiment at Jefferson Lab using a transversely- as well as longitudinally-polarized frozen-spin target.^{15,16} In particular, we will be able to measure three single-polarization observables (P_x , P_y , P_z) and nine double-polarization observables ($P_x^{c,s}$, $P_y^{c,s}$, $P_z^{c,s}$, P_x^\odot , P_y^\odot , and P_z^\odot) in the mass range up to $2 \text{ GeV}/c^2$. Figure 8 shows as an example predictions of the double-polarization observable P_z^\odot from the model of Fix and Arenhövel along with expected uncertainties of the proposed data. The data will be able to differentiate between various assumptions in the reaction dynamics; here, the question of the s - and d -wave decay of the $N(1520)$ resonance into $\pi\Delta$.

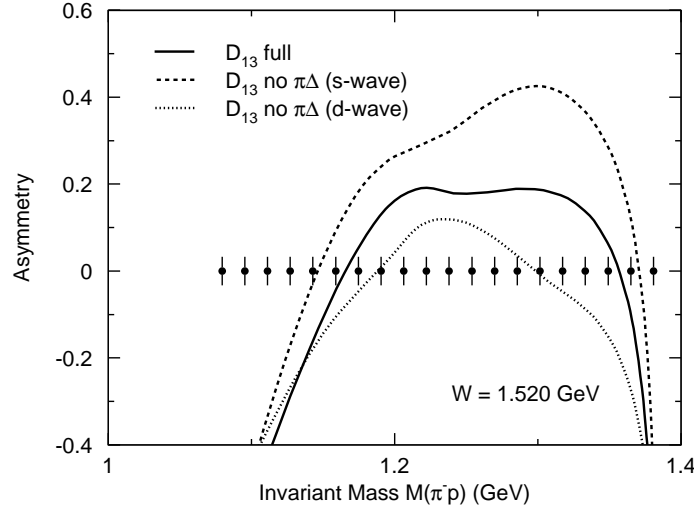


Figure 8. Predictions of the double-polarization observable P_z^\odot in the $\bar{\gamma}p \rightarrow p\pi^+\pi^-$ reaction with circularly polarized photon beam and longitudinally polarized target at $W = 1.520$ GeV. The curves show results from a model by Fix and Arenhövel¹¹ for the full model (solid) and assuming no s -wave decay (dashed), or no d -wave decay (dotted) of the $N(1520)$ resonance. The points indicate the uncertainties which could be achieved in a proposed frozen-spin target experiment at CLAS.¹⁵

Additional constraints for models or partial-wave analyses are provided by recent studies of the $\gamma p \rightarrow \pi^0\pi^0p$ reaction channel, and are particularly expected from new double-polarization experiments planned at ELSA.¹⁷

In summary, we have given a brief overview of our $\bar{\gamma}p \rightarrow p\pi^+\pi^-$ data, and we have demonstrated, by means of phenomenological models, the sensitivity of this helicity-asymmetry observable to the dynamics of the reaction. Although existing phenomenological models do describe unpolarized cross sections in the double-pion photo- and electroproduction reaction, they have severe shortcomings in the description of the beam-helicity asymmetries. In the region of overlapping nucleon resonances (and model dependent backgrounds), it clearly will be a challenge to any theoretical model to describe this and other new observables from future experiments that depend so sensitively on the interferences between them. Yet, without a proper understanding of the $\pi\pi N$ channel the problem of the “missing” resonances is unlikely to be resolved.

5. Acknowledgments

This work was supported by the Italian Istituto Nazionale di Fisica Nucleare, the French Centre National de la Recherche Scientifique and Commissariat à l'Energie Atomique, the U.S. Department of Energy and National Science Foundation, and the Korea Science and Engineering Foundation. Southeastern Universities Research Association (SURA) operates the Thomas Jefferson National Accelerator Facility under U.S. Department of Energy contract DE-AC05-84ER40150.

References

1. S. Eidelman *et al.*, Phys. Lett. **B592**, 1 (2004).
2. S. Capstick and W. Roberts, Phys. Rev. D **49**, 4570 (1994).
3. ABBHHM Collaboration, Phys. Rev. **175**, 1669 (1968); ABBHHM Collaboration, Phys. Rev. **188**, 2060 (1969); A. Braghieri *et al.*, Phys. Lett. **B363**, 46 (1995); F. Härter *et al.*, Phys. Lett. **B401**, 229 (1997); M. Wolf *et al.*, Eur. Phys. J. **A9**, 5 (2000); Y. Assafiri *et al.*, Phys. Rev. Lett. **90**, 222001 (2003); M. Ripani *et al.*, Phys. Rev. Lett. **91**, 022002 (2003); S. A. Philips, Ph.D. thesis, The George Washington University (2003); M. Bellis, Ph.D. thesis, Rensselaer Polytechnic Institute (2003); W. Langgärtner *et al.*, Phys. Rev. Lett. **87**, 052001 (2001).
4. J. Ballam *et al.*, Phys. Rev. D **5**, 545 (1972); J. Ahrens *et al.* (GDH and A2 Collaborations), Phys. Lett. **B551**, 49 (2003).
5. S. Strauch *et al.* (CLAS Collaboration), Phys. Rev. Lett. **95**, 162003 (2005).
6. W. Roberts and T. Oed, Phys. Rev. **C 71**, 055201 (2005); W. Roberts, these Proceedings.
7. B. A. Mecking *et al.*, Nucl. Instrum. Methods **A503**, 513 (2003).
8. D. I. Sober *et al.*, Nucl. Instrum. Methods **A440**, 263 (2000).
9. H. Olsen and L. C. Maximon, Phys. Rev. **114**, 887 (1959).
10. V. I. Mokeev *et al.*, Yad. Fiz. **64**, 1368 (2001), [Phys. At. Nucl. **64**, 1292 (2001)]; V. Burkert *et al.*, Nucl. Phys. **A737**, S231 (2004); V. I. Mokeev *et al.*, Proc. NSTAR2004 (World Scientific, New Jersey, 2004), p. 321; V. I. Mokeev, these Proceedings.
11. A. Fix and H. Arenhövel, Eur. Phys. J. A **25**, 115 (2005).
12. T.N. Ukwatta *et al.*, submitted to the Proceedings of the “VI Latin American Symposium on Nuclear Physics and Applications”, Iguazú, Argentina (2005).
13. L. Roca, Nucl. Phys. **A748**, 192 (2005).
14. S. Strauch *et al.*, Proc. NSTAR2004 (World Scientific, New Jersey, 2004), p. 317.
15. Jefferson Lab proposal P06-013, “Measurement of $\pi^+\pi^-$ Photoproduction in Double-Polarization Experiments using CLAS”, M. Bellis, V. Credé, S. Strauch, spokespeople.
16. F. Klein, these Proceedings.
17. U. Thoma, these Proceedings.